NASA TECHNICAL MEMORANDUM

NASA TM X-73600

NASA TM X-73600

GASEOUS SODIUM SULFATE FORMATION IN FLAMES AND FLOWING GAS ENVIRONMENTS

by Carl A. Stearns Robert A. Miller, Fred J. Kohl,
and George C Fryburg
Lewis Research Center
Cleveland, Ohio 44135

TECHNICAL PAPER to be presented at the
Symposium on Corrosion Problems Involving Volatile Corrosion Products
sponsored by the Electrochemical Society
Philadelphia, Pennsylvania, May 8-13, 1977

GASEOUS SODIUM SULFATE FORMATION IN FLAMES AND FLOWING GAS ENVIRONMENTS

by Carl A. Stearns, Robert A. Miller,* Fred J. Kohl and George C. Fryburg

National Aeronautics and Space Administration
Lewis Research Center
Cleveland, Ohio 44135

E-9029

ABSTRACT

Formation of $Na_2SO_4(g)$ in flames and hot flowing gas systems was studied by high pressure, free-jet expansion, modulated molecular beam mass spectrometric sampling. Fuel-lean CH_4-O_2 flames doped with SO_2, H_2O and NaCl yielded the gaseous Na_2SO_4 molecule in residence times of less than one millisecond. Intermediate species $NaSO_2(g)$ and $NaSO_3(g)$ were also observed and measured. Composition profiles were obtained for all reaction products. Non-flame flowing gas experiments showed that Na_2SO_4 and $NaSO_3$ gaseous molecules were formed at 1140° C in mixtures of O_2, $H_2O(g)$, SO_2 and NaCl(g). Experimental results are compared with calculated equilibrium thermodynamic predictions.

INTRODUCTION

It is well recognized that sodium sulfate is one of the major reactants involved in the hot corrosion process which can take place in turbine engines (Refs. 1 - 3). However, there is considerable speculation regarding the kinetics of the gas phase formation of sodium sulfate and the mechanism by which condensed sodium sulfate appears on hot gas path engine parts

*NRC Resident Research Associate.

STAR Category 26

(Refs. 4 and 5). Generally, it has been assumed that sulfur impurities in the fuel and sodium chloride contained in the ingested air react during combustion to yield gaseous sodium sulfate (Refs. 1 and 4). The $Na_2SO_4(g)$ has been postulated to condense on hot engine parts under certain specific conditions (Refs. 6 and 7). The most commonly proposed overall reactions for the formation of $Na_2SO_4(g)$ are (Refs. 1, 4, and 6):

$$2NaCl(g) + SO_2(g) + \frac{1}{2} O_2(g) + H_2O(g) = Na_2SO_4(g) + 2HCl(g) \qquad (1)$$

$$2NaOH(g) + SO_2(g) + \frac{1}{2} O_2(g) = Na_2SO_4(g) + H_2O(g) \qquad (2)$$

Our recent high temperature Knudsen cell investigation of the vaporization of sodium sulfate (Ref. 7) has lent credence to such reactions by establishing the existence of the $Na_2SO_4(g)$ molecule and by providing values for its thermodynamic properties. Using the data for $Na_2SO_4(g)$ and other pertinent molecular species (including NaCl(g), NaOH(g), $SO_2(g)$, $SO_3(g)$, and HCl(g)), we were able to obtain thermodynamic descriptions of the equilibria possible in various combustion systems of practical interest (Ref. 7). The results of such calculations predict that under equilibrium conditions sodium sulfate will be formed in burner rigs and turbine engines operating with anticipated environmental parameters. The objective of the research reported here was to investigate the kinetics of $Na_2SO_4(g)$ formation in dynamic systems and to compare experimental findings with calculated equilibrium predictions for the systems studied. Such information should provide some indication of how well equilibrium calculations could be applied to turbine engines.

EXPERIMENTAL

Two experimental systems were used to study the formation of $Na_2SO_4(g)$. The first system consisted of atmospheric pressure, fuel-lean, methane-oxygen flames doped with SO_2, H_2O, and NaCl. The second system consisted of a reaction tube apparatus in which atmospheric pressure flowing

mixtures of gaseous O_2, SO_2, H_2O and NaCl were heated. For both systems, high pressure mass spectrometric sampling was used to identify and measure gas phase reactants and reaction products. In the respective experiments with each system, the burner or reaction tube apparatus was appropriately positioned at the inlet orifice of the sampler. Methane-oxygen flames were produced with the burner shown in Figure 1 by mixing the gases in the mixing chamber and flowing the mixture through a series pair of 2.5 cm diameter (4.20 cm^2 open area) by 1.25 cm long flow-straighteners. (All flow straighteners were honeycombs fabricated from the alloy Hastelloy X, and the honeycomb openings were 0.08 cm on a side with about 135 openings per square centimeter.) Upon ignition, the combustible mixture burned in a plane slightly above the top flow straightener. The premixed, laminar-flow, flat flame was screened from the ambient atmosphere by a circumferential laminar flow of nitrogen emanating from a flow straightener around the water cooled combustible mixture flow pipe. The screen gas flow straightener was 1.25 cm long with inside and outside diameters of 2.5 and 5 cm, respectively. Flames were doped by adding SO_2 to the mixing chamber and by nebulizing aspirated solutions of NaCl + H_2O into the mixing chamber. Gas flow rates were regulated with needle valves and measured with calibrated rotometers. Nebulization rates were determined by measuring the rate of solution aspiration and the rate of return of liquid recovered from the mixing chamber. For typical gas flow rates used in this study, a flat flame similar to those shown in Figure 2 was obtained. The flame had a luminous zone thickness of about one millimeter, and the flame was located somewhat less than one millimeter above the top surface of the burner.

The burner was supported by mechanical devices which facilitated micrometer movement in three mutually perpendicular directions. The vertical distance, perpendicular to the flame front, between the sampler inlet orifice and surface of the burner is denoted as Z. The distance Z was varied in the range from 0.3 to 12 mm and measured with a precision of 0.025 mm.

The apparatus for the second system is shown schematically in Figure 3. A quartz reaction tube with an inside diameter of 2.2 cm was supported inside a 15 cm long tube furnace. The reaction zone temperature was controlled by a current proportionating, precision set-point, temperature controller whose primary element was a Pt-Pt 13 % Rh thermocouple in contact with the outside of the reaction tube at the midpoint of the furnace height. The reaction zone temperature was measured with a separate Pt-Pt 13 % Rh thermocouple, sheathed in alumina up to the junction, located inside the reaction tube. Temperature control in the reaction zone was $\pm 2^{o}$ C. Sodium chloride gas was generated by heating NaCl(c) contained in a 0.6 cm diameter platinum crucible. The crucible was supported on an alumina double bore tube which sheathed a Pt-Pt 13 % Rh thermocouple whose junction contacted the bottom of the crucible. The crucible and its support were located inside a 1.3 cm diameter quartz tube which was inside the reaction tube and which extended up to about 6 cm from the top of the reaction tube. Temperature of the crucible was varied by changing its vertical position (through an O-ring slip seal) relative to furnace height.

Metered oxygen flows were supplied to the reaction tube and inner tube surrounding the platinum crucible. Metered flows of SO_2 were also supplied to the reaction tube. Water vapor was supplied to the reaction tube by bubbling its oxygen supply through water which was at room temperature. NaCl(g) concentrations were determined by measuring the weight loss of NaCl(c) in the crucible as a function of time and temperature for the flow conditions employed.

For both of the atmospheric pressure systems studied, high pressure, free-jet expansion, modulated molecular beam, mass spectrometric sampling was used to identify and measure gas phase components. The complete apparatus is shown in Figure 4. The principles of this sampling technique are detailed in the literature (Refs. 8 - 10 and references cited therein). Our sampler, as shown schematically in Figure 5, is similar in design to the apparatus of Greene and Milne (Refs. 11 and 12). Atmospheric pressure gases were sampled through a 0.22 mm diameter orifice in the apex of a 0.6 cm high sampling cone which was welded to a 2 cm

diameter by 1.5 cm long stainless steel tube. The cone was fabricated from 0.25 mm thick Pt-10 % Rh and it had an included angle of 106^{o}. The expanded beam from the sampling orifice was skimmed by a skimmer cone with an orifice diameter of 0.81 mm and included angle of 60^{o}.

The distance between the sampling orifice and skimmer orifice was 3.17 cm. For this physical configuration, with the nominal pumping speeds indicated in Figure 5, first and second stage pressures were approximately 1.5×10^{-3} torr and 8×10^{-6} torr, respectively, when sampling room temperature, atmospheric pressure gas. When the gas temperature was increased to 1000^{o} C, these pressures were 7×10^{-4} torr and 1×10^{-6} torr, respectively. Third and fourth stage pressures were always less than 10^{-7} and 10^{-8} torr, respectively, for all sampling conditions. Stage I pressures were read with a capacitance manometer, and the pressures in the other three stages were read with ion gauges.

The molecular beam from the skimmer was chopped by a motor driven two-toothed chopper wheel located in Stage II. A chopping frequency of 150 hertz was used and a reference signal at this frequency was derived from a light bulb and photodiode coupled to the chopper wheel. The chopped molecular beam then passed to the electron bombardment ion source of a quadrupole mass spectrometer (Extranuclear Laboratories). The high efficiency ion source was operated with a current of approximately 3 mA of 30 eV electrons. The quadrupole filter with 1.6 cm diameter poles had a mass range extending to over 600 AMU. A Channeltron electron multiplier was employed to multiply the ion current output of the ion source-quadrupole filter. Two channels of output current were measured as a function of quadrupole filter tuning. One channel measured the total chopped ion current, and the other channel measured only the component of the ion current signal in phase with the chopper. The second channel was driven by a lock-in amplifier-phase sensitive detector system tuned to the chopper frequency reference signal.

RESULTS AND DISCUSSION

The experimental results presented here are considered to be qualitatively correct but quantitative aspects are considered preliminary. Measured ion intensities have not been adjusted to account for mass discrimination (resulting from Mach-number focusing (Refs. 8, 13, 14, and references cited therein) and quadrupole mass filter transmission (Ref. 15)) and multiplier gain variations as a function of mass-to-charge ratio, m/e. Factors such as these are best accounted for by performing in situ calibrations (e.g., see Ref. 16) and such calibrations have not yet been performed for our experiments. Ion intensities reported here have, however, been corrected for relative ionization cross sections. Cross sections for atoms were taken from Mann (Ref. 17) and calculated for molecules as 0.75 times the sum of the atomic values.

Flame system. - Gaseous species in flames were measured by recording the in-phase component of the ion current for respective values of m/e. Problems of clogging of the sampler inlet orifice and the aspirator-nebulizer limited the duration of each flame experiment and thus the amount of data that could be obtained for any one flame. For this reason, the only species investigated at this time were O_2, H_2O, CO_2, SO_2, Na, NaCl, HCl, $NaSO_2$, $NaSO_3$, and Na_2SO_4. These molecules were monitored by measuring the ion intensities for the respective molecular ions. We assume that $NaSO_2^+$ and $NaSO_3^+$ are parent ions from the molecules $NaSO_2$ and $NaSO_3$ rather than fragments because these species were not observed in the Knudsen cell vaporization of sodium sulfate (Ref. 7). Furthermore, several investigators (Refs. 18 and 19) have indicated that $NaSO_2(g)$ and $NaSO_3(g)$ are to be expected in suitably doped flames.

For all species investigated, the ion intensity was measured as a function of the distance Z for a 9.5 mole ratio O_2/CH_4 flame doped with SO_2, NaCl, and H_2O. Measured composition profiles for this flame are presented in Figure 6. Weight percentages of reactants in the flame were 4.7 CH_4, 89.4 O_2, 3.5 H_2O, 2.0 SO_2, and 0.35 NaCl. The flame speed, calculated on the basis of the STP flow velocities of the reactant gases, was

42 cm sec^{-1}. No attempt was made to make intensity measurements at values of Z less than 0.3 mm. In the course of investigation it was observed that at small values of Z the sampling cone appeared to perturb the flame. Attachment of the flame to the sampling cone appeared to take place at approximately Z = 0.8 mm where a decrease in total ion intensity was observed. The ramifications of various flame-sampling probe interactions have been considered in detail by Biordi et al. (Refs. 20 and 21). The composition profiles shown in Figure 6 indicate that $Na_2SO_4(g)$, $NaSO_2(g)$, and $NaSO_3(g)$ are formed very early in the flame. Residence times were calculated on the basis of flow velocities determined for the total flow of unreacted cold gas. On this basis we estimate that the species $Na_2SO_4(g)$, $NaSO_2(g)$, and $NaSO_3(g)$ are formed in residence times of less than one millisecond.

The composition profiles obtained for the species O_2, H_2O, and CO_2 are generally similar to those reported for CH_4-O_2 flames (Ref. 22). For the other sodium- and sulfur-containing species, except $Na_2SO_4(g)$, the observed profile shapes seem reasonable and can be rationalized in general terms. However, the drop in intensity, with increasing Z from the peak, exhibited by the $Na_2SO_4(g)$ profile is unexpected. We speculate that the $Na_2SO_4(g)$ profile may be the result of several inter-related factors such as: (1) cooling of the flame by the sampling cone (the stability of $Na_2SO_4(g)$ increases with decreasing temperature), (2) actual variation of flame temperature as a function of Z, and (3) existence of a region of supersaturation for this species.

The species $NaSO_2(g)$ and $NaSO_3(g)$ have profiles whose shapes are generally similar to $Na_2SO_4(g)$ but the intensity of these species was found to decrease to values below our detection sensitivity for distances greater than about Z = 1.2 mm. The profile shapes for $NaSO_2(g)$ and $NaSO_3(g)$ may be the result of the same factors accounting for the $Na_2SO_4(g)$ profile. On the other hand, elevated concentrations of $NaSO_2$ and $NaSO_3$ could have led to higher concentrations of Na_2SO_4 if they were intermediates which were rapidly converted to Na_2SO_4.

To facilitate a comparison of experimental observations with equilibrium thermodynamic predictions we calculated the mole fractions of flame reaction products. The calculations were performed with the NASA complex chemical equilibrium computer program (Ref. 23) which has been described in detail previously. This program is based on the minimization of free energy approach to chemical equilibrium calculations subject to the constraint of maintaining a proper mass balance between reactants and products. The program permits the calculation of chemical equilibrium composition for homogeneous or heterogeneous systems for assigned thermodynamic states such as temperature-pressure (T, P) and enthalpy-pressure (H, P). For the present work, the role of Na_2SO_4 (c or g) in typical doped methane-oxygen flames was examined by obtaining results describing flame temperatures and compositions as a function of fuel-to-oxidant mass ratio. For the calculations, the convention used was that CH_4 and SO_2 were labeled fuel and O_2, H_2O, and NaCl were labeled oxidant. The equilibrium compositions of the reacted flame gases at the adiabatic flame temperatures are presented in Figure 7(a) for the major products and in Figure 7(b) for the sodium-containing species. To arrive at the distribution of molecular species depicted in these figures, the program considered over 70 gaseous and condensed species made up of C-H-O-S-Na-Cl combinations. A list of the species considered is given in Table I. The thermodynamic data for most of these species was obtained from the JANAF tables (Ref. 24), while the data for Na_2SO_4(g) were taken from Ref. 7. It must be pointed out that only those molecular species for which the program was given thermodynamic data were considered in the calculations; no data for $NaSO_2$ or $NaSO_3$ were included.

The results of the calculations show that the sodium is distributed in a complex pattern between Na_2SO_4(c), NaCl(g), NaOH(g), Na_2SO_4(g) and Na(g). At low values of the fuel/oxidant ratio (corresponding to low flame temperatures) and up to a sharp cut off point, the sodium is tied up almost exclusively as Na_2SO_4(c). Gaseous Na_2SO_4 is present in significant amounts over a relatively narrow fuel/oxidant ratio range and is always present at a molar concentration of less than 10 % of NaCl(g). At high fuel/oxidant ratios, NaOH(g), Na(g), and NaCl(g) account for most of the sodium.

Experimental results can be compared with the calculations by noting that, according to the fuel and oxidant convention used, the fuel/oxidant mass ratio for the experimental flame was 0.072. For ease of comparison, calculated mole fractions of product species for the ratio 0.072 are shown on the right-hand side of Figure 6. At the outset one must recognize that two factors prevail: (1) as noted earlier, the experimental results were not "calibrated," and (2) the calculations are for equilibrium conditions. With these factors in mind, the agreement between experiment and calculation is considered to be good for the species O_2, H_2O, CO_2, SO_2, and SO_3, all of which are only slowly varying functions of the fuel/oxidant ratio. For the remaining experimentally measured species other factors must be considered. These factors include: (1) the fuel/oxidant ratio given for the experimental flame has uncertainty associated with it due mainly to the method used to introduce the sodium chloride, (2) most of the sodium- and sulfur-containing species are critically dependent on the fuel/oxidant ratio, (3) the stability of $Na_2SO_4(g)$ is a rapidly varying function of temperature, and (4) the experimental flame temperature is expected to be significantly below the calculated adiabatic flame temperature of 2032 K (Ref 25). We calculate that if the flame were 200° cooler the predicted level of $Na_2SO_4(g)$ would equal the experimental level. By reflecting on all the factors to be considered, we conclude that the agreement between experiment and calculation is reasonable and that the calculations are useful in predicting at least qualitatively what is to be expected in experimental flame systems.

That the $Na_2SO_4(g)$ species, predicted by the calculations, was observed experimentally in short residence times is of fundamental significance to the hot corrosion problem. Our observations regarding the formation of $Na_2SO_4(g)$ are considerably different from Hanby's (Ref. 5) finding that residence times of about 8 milliseconds are required for the formation of sodium sulfate. While Hanby's results are for a different experimental system, we would predict from equilibrium calculations that for his case of 5 % excess air (i.e., a fuel/air ratio of about 0.056) $Na_2SO_4(g)$ would not be expected to form. We have made experimental measurements of $Na_2SO_4(g)$ formation at various fuel/oxidant ratios and the results generally were in agreement with the calculated shape of the $Na_2SO_4(g)$ mole fraction versus

fuel/oxidant ratio curve. Obviously, further consideration is needed to resolve the differences between our observations on the formation of $Na_2SO_4(g)$ and the observations of Hanby.

Reaction tube system. - For these experiments the quartz reaction tube apparatus was positioned at the inlet to the sampler so that the sampling cone extended down into the reaction zone. The sampling cone was allowed to reach temperature (due to heat conduction its temperature was probably somewhat lower than the reaction zone temperature) before experiments were initiated. When water-saturated oxygen, SO_2 and NaCl(g) were flowed through the reaction zone which was at 1413 K, the species $Na_2SO_4(g)$ and $NaSO_3(g)$ were observed. The species $NaSO_2(g)$ was not observed in these experiments. The species $Na_2SO_4(g)$ and $NaSO_3(g)$ could be made to vanish almost instantly by cutting off the supply of SO_2. When the supply of NaCl(g) was removed (by cooling the platinum crucible containing NaCl(c)), these species slowly disappeared. The species $NaSO_3(g)$ persisted when only the supply of water vapor was removed but the species $Na_2SO_4(g)$ disappeared completely. This is additional evidence that $NaSO_3^+$ is a parent molecular ion and not a fragment from Na_2SO_4 because it was observed under conditions where Na_2SO_4 was not present.

Intensities were measured for the gaseous species O_2, H_2O, SO_2, SO_3, NaCl, Na_2SO_4, and $NaSO_3$ with known flows of O_2, SO_2, H_2O and known concentrations of NaCl(g). The species NaOH(g) and HCl(g) with parent ions at m/e 40 and 36, 38 could not be measured because large in-phase background peaks were present at these m/e values. These background peaks were due to argon which is a 2300 ppm impurity in the missile grade oxygen that was used.

Equilibrium thermodynamic calculations of the composition of the reaction products were made as a function of temperature. In the calculations the composition of the reactants was held constant at the weight fractions 0.96 O_2, 1.2×10^{-5} NaCl, 0.012 H_2O, and 0.032 SO_2. Calculated reaction products as a function of temperature are presented in Figure 8. Again it is to be noted that $Na_2SO_4(g)$ is predicted as a reaction product at observable concentrations. Experimental results are compared with the results

of calculations in Table II. Considering that the measured intensities were not corrected for sampling factors, the quality of agreement between experiment and calculation is considered quite good.

Although the data shown in Table II indicate good agreement between experiment and equilibrium calculations, it seemed desirable to assess independently how close the experimental conditions approached equilibrium conditions. The reaction $SO_2(g) + \frac{1}{2} O_2(g) = SO_3(g)$ provides a basis for such an assessment. At temperatures below about 1050 K, SO_3 is more stable than SO_2 in O_2 but the rate of conversion of SO_2 to SO_3 is known to be very slow at temperatures below about 1370 K (Ref. 26). Experimentally, we measured the relative concentrations of the SO_2 and SO_3 molecules as a function of temperature when a few percent of SO_2 was added to one atmosphere of O_2 flowing in the reaction tube. The intensity ratio SO_3/SO_2 (corrected only for cross sections) was taken to be the equilibrium constant for the reaction. Residence times within the hot section of the tube were about 2 seconds. In Figure 9 the experimental equilibrium constants are plotted as a function of reciprocal temperature. The calculated line is from the literature (Ref. 24). In another experiment the reaction was catalysed by passing the gas mixture over a ball of fine platinum wire, and the resulting equilibrium constants are also plotted in this figure. In each case the slope of the experimental curves approached that of the calculated curves at higher temperatures. From this one can conclude that for the temperature at which the formation of Na_2SO_4 was investigated (1413 K), equilibrium was established between the SO_2 and SO_3 components of the reaction system.

CONCLUDING REMARKS

In summary, we have observed the formation of gaseous Na_2SO_4 and $NaSO_3$ in both atmospheric pressure flames and in a flowing gas mixture. In addition, $NaSO_2$(g) was observed in flames. The measurements show that Na_2SO_4(g) can be formed in reaction times of less than one millisecond from SO_2-, H_2O-, and NaCl-doped flames. The formation and behavior as a function of fuel/oxidant ratio of Na_2SO_4(g) in flames is in qualitative agreement with equilibrium thermochemical predictions.

REFERENCES

1. J. Stringer, Metals Ceramic Information Center, Columbus, Oh, MCIC 72-08 (1972).

2. N. S. Bornstein, M. A. DeCrescente, and H. A. Roth, in "Proceedings of the 1972 Tri-Service Conference on Corrosion," MCIC 73-19, M. M. Jacobson and A. Gallaccio, Editors, p. 15, Metals and Ceramic Information Center, Columbus, Oh (1973).

3. J. A. Goebel, and F. S. Pettit, in "Metal-Slag Gas Reactions and Processes," Ed. by Z. A. Foroulis and W. W. Smeltzer, Editors, p. 693, The Electrochem. Soc., Princeton, N.J. (1975).

4. J. F. G. Condé, in "High Temperature Corrosion of Aerospace Alloys," AGARD CP-120, J. Stringer, R. I. Jaffee and T. F. Kearns, Editors, p. 204, Advisory Group for Aerospace Research and Development, France (1972).

5. V. I. Hanby, J. Eng. Power 96, 129 (1974).

6. N. S. Bornstein, and M. A. DeCrescente, Corrosion 24, 127 (1968).

7. F. J. Kohl, C. A. Stearns, and G. C. Fryburg, in "Metal-Slag Gas Reactions and Processes," Z. A. Foroulis and W. W. Smeltzer, Editors, p. 649, The Electrochem. Soc., Princeton, N.J. (1975).

8. J. B. Anderson, in "Molecular Beams and Low Density Gas Dynamics," P. P. Wegener, Editor, p. 1, Marcel-Dekker, Inc., New York (1974).

9. J. B. Anderson, R. P. Andres, and J. B. Fenn, in "Advances in Atomic and Molecular Physics," Vol. 1, O. R. Bates and I. Estermann, Editors, p. 345, Academic Press, N.Y. (1965).

10. T. A. Milne, and F. T. Greene, in "Advances in High Temperature Chemistry," Vol. 2, L. Eyring, Editor, p. 107, Academic Press, New York (1969).

11. F. T. Greene, and T. A. Milne, in "Advances in Mass Spectrometry," Vol. 3, W. L. Mead, Editor, p. 841, The Institute of Petroleum, London (1966).

12. T. A. Milne, and F. T. Greene, J. Chem. Phys. 44, 2444 (1966).

13. T. A. Milne, J. Brewer, and F. T. Greene, in "Proceedings of the First Meeting of the Interagency Chemical Rocket Propulsion Group, Working Group on Thermochemistry," Vol. 1, CPIA-44, p. 123, Chemical Propulsion Information Agency, Silver Spring, Md. (1964).

14. P. K. Sharma, E. L. Knuth, and W. S. Young, J. Chem. Phys. 64, 4345 (1976).

15. T. C. Ehlert, J. Phys. E:Sci, Inst. 3, 237 (1970).

16. J. C. Biordi, C. P. Lazzara, and J. F. Papp, Bureau of Mines, Pittsburgh, Pa., BM-RI-7723 (1973).

17. J. B. Mann, in "Recent Developments in Mass Spectrometry," K. Ogata and T. Hayakawa, Editors, p. 814, Univ. Press, Baltimore, Md. (1970).

18. C. P. Fenimore, in "Fourteenth International Symposium on Combustion," p. 955, The Combust. Inst. Pittsburg, Pa. (1973).

19. R. A. Durie, G. M. Johnson, and M. Y. Smith, in "Fifteenth International Symposium on Combustion." p. 1123, The Combust. Inst. Pittsburg, Pa. (1975).

20. J. C. Biordi, C. P. Lazzara, and J. F. Papp, Combust. Flame 23, 72 (1974).

21. J. C. Biordi, C. P. Lazzara, and J. F. Papp, Combust. Flame 26, 57 (1976).

22. J. Peeters and G. Mahnen, in "Fourteenth International Symposium on Combustion," p. 133, The Combust. Inst., Pittsburg, Pa. (1973).

23. S. Gordon and B. J. McBride, NASA SP-273 (1971).

24. JANAF Thermochemical Tables, Dow Chemical Co., Midland, Mich.

25. T. A. Milne, Air Force Materials Lab., Wright-Patterson AFB Oh, AFML-TR-69-225 (1969).

26. Cullis, C. F. and Mulcahy, M. R. F., Combust. Flame 18, 225 (1972).

TABLE I. - SPECIES CONSIDERED IN COMPUTER CALCULATIONS

(PHASES LISTED WITHOUT PARENTHESES ARE GASES)

C(S)	C_4	Na_2Cl_2
C	C_5	$Na_2O(c)$
CCl	Cl	Na_2O
CCl_2	ClO	$Na_2(OH)_2$
CCl_3	ClO_2	$Na_2S(c)$
CCl_4	Cl_2	$Na_2SO_4(c)$
CH	Cl_2O	Na_2SO_4
CH_2	H	O
CH_2O	HCl	OH
CH_3	HCO	O_2
CH_4	HO_2	O_3
CH_4O	H_2	S(c)
CO	$H_2O(c)$	S
COCl	H_2O	SF
$COCl_2$	H_2O_2	SO
COS	H_2S	SO_2
CO_2	$H_2SO_4(c)$	SO_2Cl_2
CS	H_2SO_4	SO_3
CS_2	Na(c)	S_2
C_2	Na	S_8
C_2Cl_2	NaCl(c)	
C_2H	NaCl	
C_2H_2	NaH	
C_2H_4	NaO	
C_2H_6	NaOH(c)	
C_2O	NaOH	
C_3	Na_2	
C_3O_2	$Na_2CO_3(c)$	

TABLE II. - FORMATION OF Na_2SO_4 IN A FLOWING GAS MIXTURE AT 1413 K

Molecule	Experimental ion intensity fraction	Equilibrium calculation of mole fraction
O_2	0.98	0.96
H_2O	1.3×10^{-2}	2.2×10^{-2}
SO_2	1.0×10^{-2}	1.5×10^{-2}
SO_3	3.3×10^{-4}	9.0×10^{-4}
NaCl	8.7×10^{-6}	3.4×10^{-6}
Na_2SO_4	9.0×10^{-7}	1.4×10^{-6}
$NaSO_3$	1×10^{-7}	------

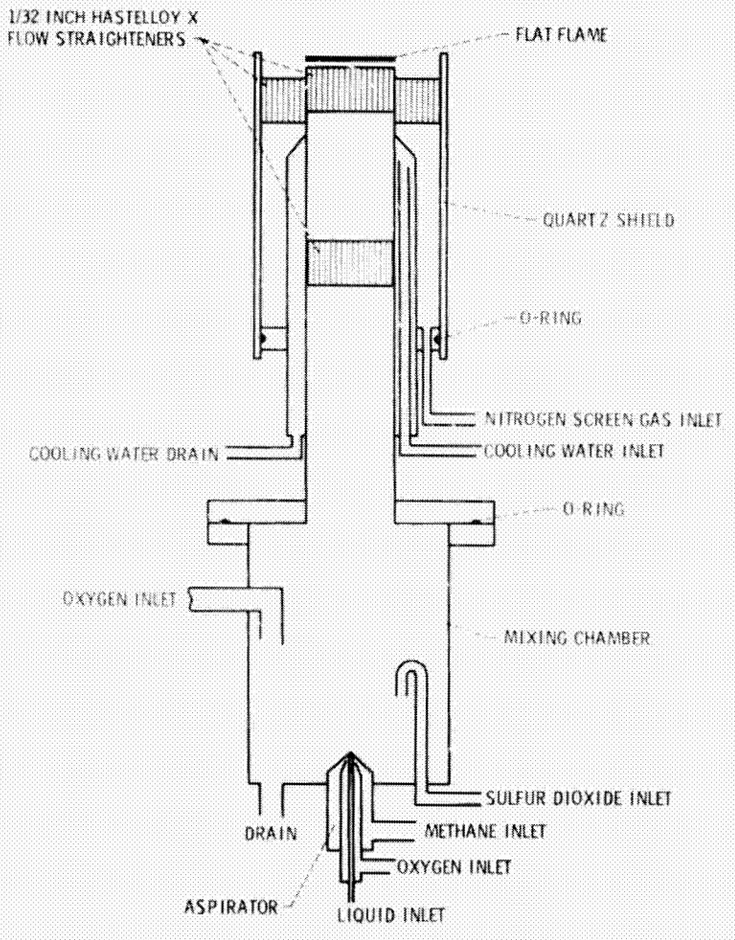

Figure 1. - Schematic of flat flame burner.

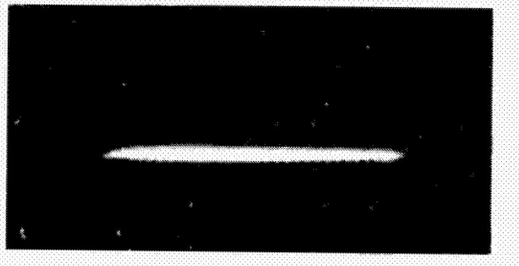

(a) WITHOUT NaCl.

(b) WITH NaCl.

Figure 2. - Flame.

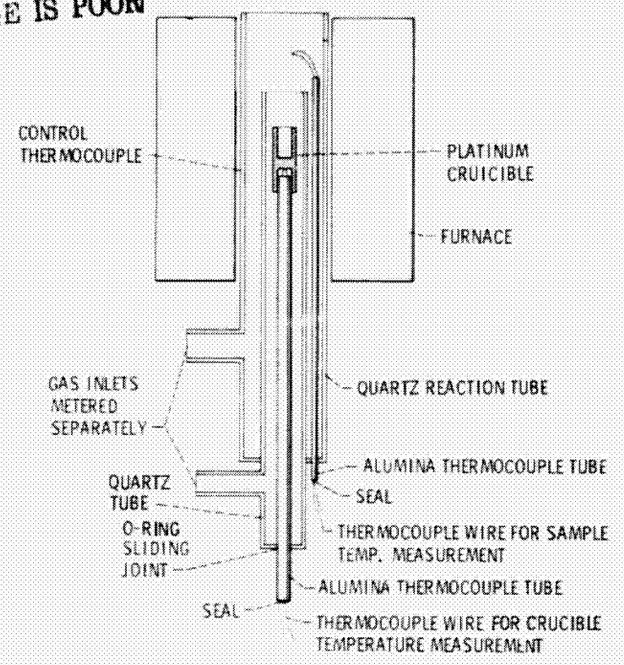

Figure 3. - Schematic of reaction tube apparatus.

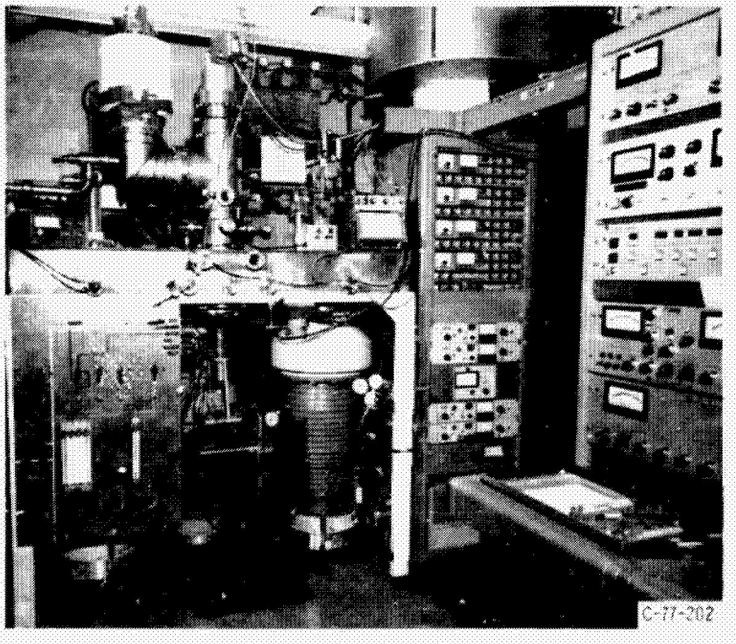

Figure 4. - Sampling system.

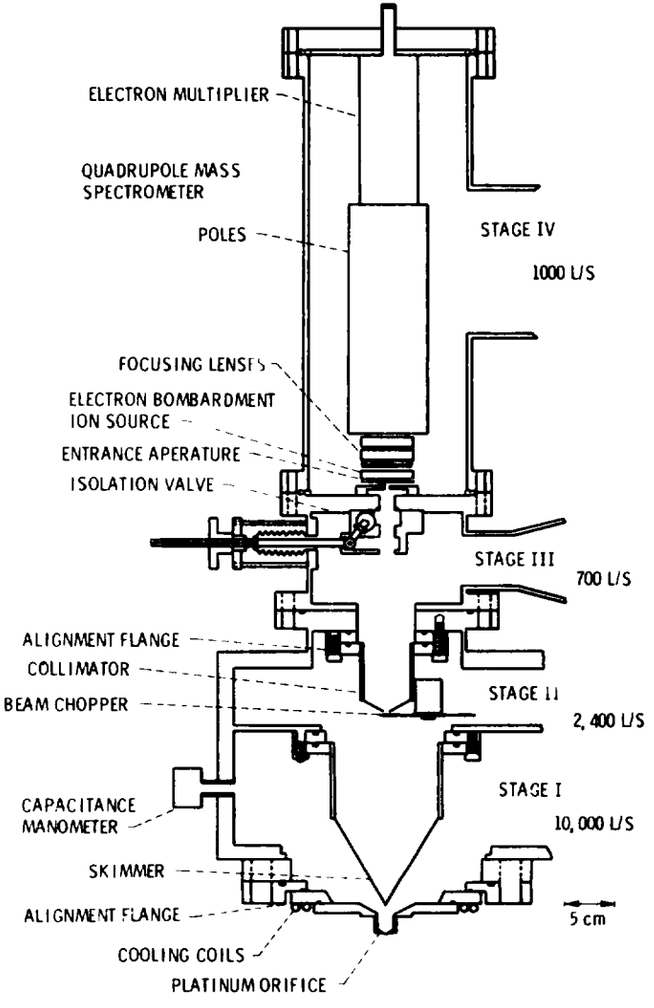

Figure 5 - Schematic of atmospheric pressure, modulated molecular beam, mass spectrometric sampler

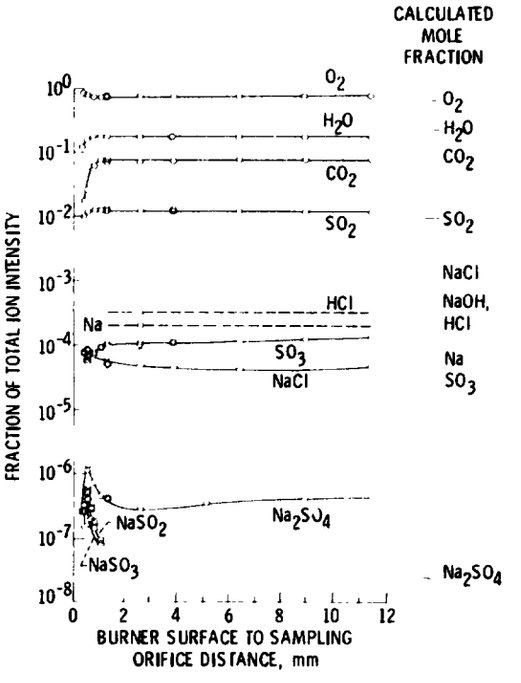

Figure 6. - Composition profiles for CH_4-O_2-H_2O-NaCl-SO_2 flame. Reactants (wt.%): CH_4, 4.7; O_2, 89.4; H_2O, 3.5; SO_2, 2.0; and NaCl, 0.35.

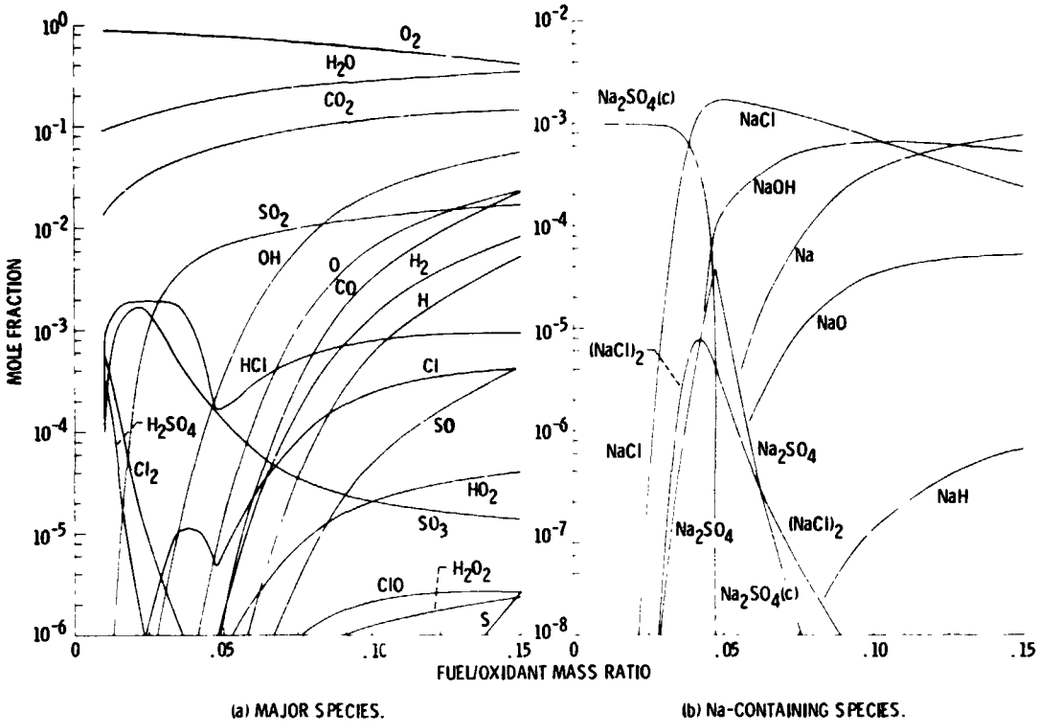

(a) MAJOR SPECIES. (b) Na-CONTAINING SPECIES.

Figure 7. - Equilibrium chemical composition of flame gas versus fuel/oxidant ratio of CH_4-O_2 flame doped with NaCl and SO_2.

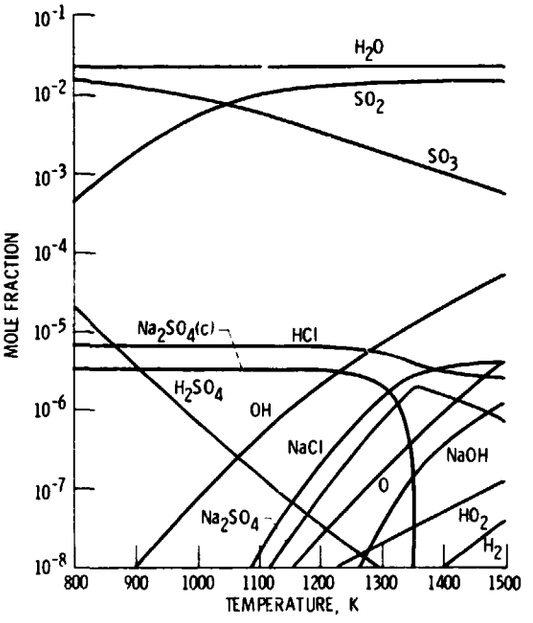

Figure 8. - Equilibrium composition of the Na-S-O-H-Cl system as a function of temperature. Reactant (wt. fraction): O_2, 0.96; SO_2, 0.032; H_2O, 0.012; and NaCl, 1.2×10^{-5}.

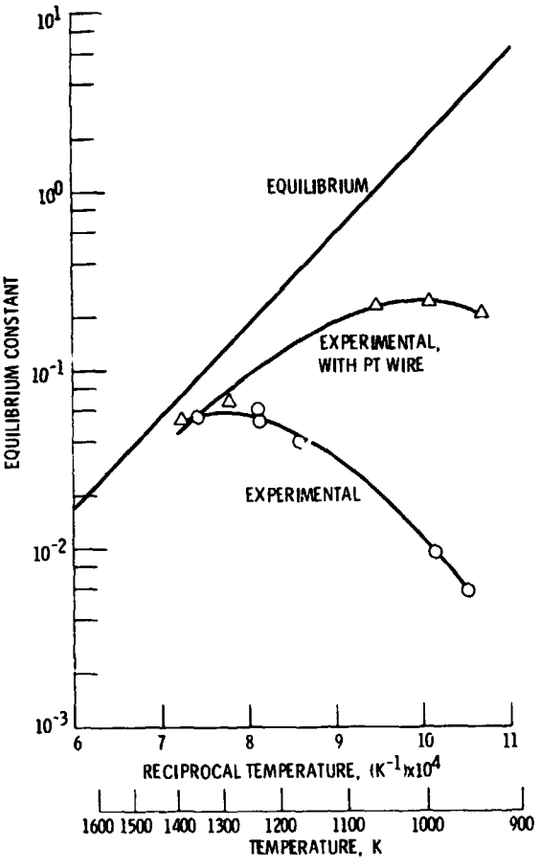

Figure 9. - Equilibrium constant versus temperature for the reaction $SO_2(g) + \frac{1}{2} O_2(g) = SO_3(g)$.